

Simultaneous ionization and excitation of Ar by electrons with particular attention to configuration-interaction effects*

K-H. Tan and J. W. McConkey

Department of Physics, University of Windsor, Windsor, Ontario, Canada

(Received 11 June 1974)

Absolute apparent cross sections for electron impact excitation of the $4s'$, $5s$, $3d$, $4d$, $5d$, $3d'$, and $4d'$ configurations of Ar^+ from the ground state of Ar are presented by studying the vacuum uv photon decay of the states. The high-energy behavior of the excitation functions is demonstrated to reflect the two-electron nature of the initial excitation. Where cascade can be satisfactorily taken into account, excitation of states with the same orbital angular momentum and multiplicity is shown to be according to their statistical weights. Some significant discrepancies are exposed between theoretically calculated and experimentally measured relative transition probabilities. Configuration-interaction effects are demonstrated to exist in a number of instances and are quantitatively investigated for the ${}^2S_{1/2}$ states.

INTRODUCTION

Recent papers from this laboratory have reported on a variety of phenomena associated with electron impact on the argon atom. Measurements have been reported on total ionization cross sections,¹ autoionization effects,² elastic scattering,³ excitation of the resonance lines,⁴ and some one- and two-electron processes leading to excited states of the ion.⁵ The present paper presents data on the simultaneous ionization and excitation of the atom to various configurations of the ion and particular attention is paid to the role of configuration interaction in this process. The cross sections which are presented should be valuable in elucidating the relative importance of various processes occurring in the Ar-ion laser and also for calibration purposes in vacuum uv spectroscopy.

Figure 1 is a simplified term diagram of Ar^+ illustrating the levels studied in the present work. Configurations investigated were $3s^2 3p^4 5s$, $3s^2 3p^4 nd$ with $n=3, 4$, and 5 , $3s^2 3p^4 4s'$, $3s^2 3p^4 3d'$ and $3s^2 3p^4 4d'$. All of these configurations combine optically with the $3s^2 3p^5$ ground state of Ar^+ yielding radiation in the vacuum ultraviolet spectral region below 700 Å. The unprimed terms are based on the $3s^2 3p^4({}^3P)$ state of Ar^{++} and the primed terms are based on $3s^2 3p^4({}^1D)$ of Ar^{++} . Measurements on the $3s^2 3p^4 4s$ and $3s 3p^6$ configurations were reported previously.⁵

THEORY

The present measurements are best discussed in the context of the Bethe-Born approximation. At sufficiently high impact energies the cross sec-

tion for excitation of a level, $n\ell$, which is optically accessible from the ground state, is given by

$$\sigma(n, \ell) = 4\pi a_0^2 R E^{-1} M^2(n, \ell) \ln(CE), \quad (1)$$

where a_0 is the first Bohr radius, R the Rydberg energy, E the electron energy, C a constant, and $M^2(n\ell)$ is the square of the appropriate transition matrix element. A so-called "Bethe" plot of σE vs $\ln E$ should be a straight line at high energy with a positive slope. If the transition is optically forbidden, then the Bethe plot will have zero or negative slope at high energy. Hence from a Bethe plot one can immediately decide whether or not a particular transition is optically allowed. Optically forbidden levels can of course be readily excited when electron impact is used.

In the present instance where we are considering excitation from the ground state of neutral argon to excited levels of the ion we would expect all the levels to be optically forbidden with one exception, $3s 3p^6$, because of the fact that two-electron transitions are involved, i.e., one $3p$ electron is ejected into the continuum and another $3p$ electron is promoted to an excited level. In the case of $3s 3p^6$ a one-electron process is involved with a single $3s$ electron being ejected from the inner shell. We would expect therefore that all the Bethe plots with the exception of the plot of the $3s 3p^6$ level would have a negative slope. If other Bethe plots are found with a positive slope then we must suspect that the levels involved are linked to $3s 3p^6$ by configuration interaction. This is in fact demonstrated to be the case as outlined later.

Strong configuration-interaction effects in the argon ion were first recognized by Minnhagen⁷ in the course of a detailed investigation of the

resonance line of neon as basic standards. Previous measurements of these lines have been discussed by Donaldson *et al.*⁶ and Tan *et al.*⁵ We have used the measured values of these lines given by these workers. Future modification of these numbers would require a renormalization of this data.

Using these lines the quantum efficiency of the detection system was established at these particular wavelengths and could be interpolated to other intermediate wavelengths. Little variation in quantum efficiency was encountered. For example, the quantum efficiency was found to stay constant over the range 522–584 Å, and for this reason, the quantum efficiency at 490 Å was assumed to be the same as at 522 Å. This should introduce very little additional error in the measurements at this wavelength.

The actual comparison between two lines or groups of lines was through comparison of the slopes of intensity-pressure plots. The head pressures were measured with a Baratron capacitance manometer and beam currents were monitored using a Keithley electrometer. Negligible error is introduced in the slope comparison and so the error in the measured cross section is determined mainly by the error in the cross section of the standard line. For the helium lines this should not exceed 15% whereas for the Ne line it is somewhat larger, (20–25)%. Additional errors were introduced when the lines under consideration were not very close in wavelength to the standard line, e.g., the lines around 660 Å, when overlap of adjacent lines occurred and when low signal strengths led to appreciable statistical uncertainties. Statistical error bars are indicated on the excitation functions shown later. It is believed that the values quoted in Table I for the integrated cross section of a group of lines, are accurate to $\pm 10\%$ in addition to the possible error, mentioned above, in the standard line. The values given for the cross sections of individual lines within a group have been obtained from wavelength scans. This introduces an additional error which probably does not exceed 10% except where the lines were very closely spaced.

RESULTS AND DISCUSSION

Because of the large number of levels involved and the consequent large number of often closely spaced lines it was normally not possible to make measurements on individual lines. The procedure which was adopted to obtain the cross sections listed in Table I was to measure the integrated cross section of a group of lines and then obtain the relative cross sections of the different lines within the group by making a careful wavelength-

intensity scan using much narrower entry slits. This was sometimes a difficult procedure as illustrated in Fig. 2 which shows an intensity-wavelength scan in the 540–550 Å region together with the deconvolution to obtain the individual line profiles knowing the slit function of the monochromator. Because of the difficulties involved in such a process the quoted cross sections for closely spaced lines must be considered as only approximate. Where it was possible to measure cross sections for individual lines or pairs of lines it was found that the values obtained from the wavelength scan and the values measured directly were in close agreement. For example, the apparent cross section for excitation of the 583.4 Å ($3d'^2D_{3/2} - ^2P_{1/2}$) line at 100-eV incident electron energy, obtained from a measurement of the integrated cross section of the 572–584-Å group of lines and the associated wavelength scan, was 6.4×10^{-19} cm² while the value obtained directly was 6.1×10^{-19} cm². The difference of 5% is well within the error bars on the measurements.

Figures 3(a)–3(f) illustrate the excitation functions obtained during the course of the work. Particular attention has been paid to the $3d'$ configuration as it is the one which is expected to interact strongly with $3s3p^6$ as discussed earlier.

A number of points should be made in connection with the figures. In all cases, with the possible exception of the 486–492 Å group, the excitation functions exhibit a secondary peak or shoulder at about 60 eV in addition to the main peak which occurs at around 100 eV. As has been pointed out previously^{1,5} this structure is a feature of ionization and simultaneous ionization and excitation in Ar and is probably associated with autoionization effects. It is to be expected that the effect of autoionization would diminish as the excitation energy of the state in question became larger in agreement with the observations here.

It should be stressed that the 543–547 and the 486–492 Å excitation functions only truly represent the $3d'^2S_{1/2}$ and $4d'^2S_{1/2}$ excitation functions at the highest energies. At the lower energies the functions are mixtures of $3d'$, $4d$, and $5s$, and $4d'$ and $5d$, respectively. This is discussed more fully in the section dealing with configuration interaction.

It can be seen that in all cases with the exception of 543–547 and 486–492 Å the Bethe plots have a negative slope at high energy. The Bethe plot for the $4s$ levels presented previously⁵ also had a negative slope. This is in agreement with theoretical predictions as discussed earlier and is due to the two-electron nature of the transitions involved. This makes them dipole forbidden. The figures indicate clearly that a distinctly different excitation process is involved in the excitation of the $3d'^2S$

TABLE I. Apparent cross sections of Ar⁺ lines measured at 100-eV incident electron energy.

Wavelength (Å)	Transition	Cross section (10 ⁻¹⁹ cm ²)	Integrated cross section	
487.23	$3p^4 4d^2 S_{1/2} - 3p^5 2P_{3/2}$	4.2	15.1	
487.28	$3p^4 5d^2 P_{3/2} - 3p^5 2P_{3/2}$			
488.75	$3p^4 5d^2 D_{5/2} - 3p^5 2P_{3/2}$	5.6		
488.99	$3p^4 5d^2 P_{1/2} - 3p^5 2P_{3/2}$			
489.20	$3p^4 5d^2 D_{3/2} - 3p^5 2P_{3/2}$			
490.65	$3p^4 4d^2 S_{1/2} - 3p^5 2P_{1/2}$	4.8		
490.70	$3p^4 5d^2 P_{3/2} - 3p^5 2P_{1/2}$			
492.42	$3p^4 5d^2 P_{1/2} - 3p^5 2P_{1/2}$	0.5		
518.91	$4d^2 D_{3/2} - 2P_{3/2}$	9.1		21.1
519.33	$4d^2 D_{5/2} - 2P_{3/2}$			
522.79	$4d^2 D_{3/2} - 2P_{1/2}$	4.9		
524.68	$4d^2 P_{3/2} - 2P_{3/2}$	4.4		
526.50	$4d^2 P_{1/2} - 2P_{3/2}$	0.9		
530.49	$4d^2 P_{1/2} - 2P_{1/2}$	1.8		
542.91	$4d^4 D_{1/2} - 2P_{3/2}$	4.3		
543.21	$3d^2 S_{1/2} - 2P_{3/2}$	7.1		
543.73	$5s^2 P_{1/2} - 2P_{3/2}$	2.5		
546.18	$5s^2 P_{3/2} - 2P_{3/2}$	1.7		
547.17	$4d^4 D_{1/2} - 2P_{1/2}$	2.3		
547.46	$3d^2 S_{1/2} - 2P_{1/2}$	4.9		
547.99	$5s^2 P_{1/2} - 2P_{1/2}$	1.6		
548.78	$5s^4 P_{3/2} - 2P_{3/2}$	0.6		
550.48	$5s^2 P_{3/2} - 2P_{1/2}$	0.3		
550.896	$5s^4 P_{1/2} - 2P_{1/2}$	0.2		
572.01	$3d^2 P_{1/2} - 2P_{3/2}$	2.7		
573.36	$3d^2 P_{3/2} - 2P_{3/2}$	12.4		
576.74	$3d^2 P_{1/2} - 2P_{1/2}$	5.2		
578.11	$3d^2 P_{3/2} - 2P_{1/2}$	6.9		
578.60	$3d^2 D_{3/2} - 2P_{3/2}$			
580.26	$3d^2 D_{5/2} - 2P_{3/2}$	13.3		
583.44	$3d^2 D_{3/2} - 2P_{1/2}$	6.1		
661.87 (broad)	$3d^2 D_{5/2} - 2P_{3/2}$	8.5		
664.56	$3d^2 D_{3/2} - 2P_{3/2}$	1.2		
666.01	$3d^2 F_{5/2} - 2P_{3/2}$	3.1		
670.95	$3d^2 D_{3/2} - 2P_{1/2}$	5.9		
671.85	$4s^2 D_{5/2} - 2P_{3/2}$	14.4		
672.86	$4s^2 D_{3/2} - 2P_{3/2}$	0.6		
676.24	$3d^4 P_{5/2} - 2P_{3/2}$	1.3		
677.95	$3d^4 P_{3/2} - 2P_{3/2}$	1.1		
679.22	$3d^4 P_{1/2} - 2P_{3/2}$	9.0		
679.40	$4s^2 D_{3/2} - 2P_{1/2}$			
686.49	$3d^2 P_{3/2} - 2P_{3/2}$	1.1		
690.17 Ar III	$3d^5 D - 3p^4 P$	0.9		
691.04 (broad)	$3d^2 P_{1/2} - 2P_{3/2}$	0.8		
693.30	$3d^2 P_{3/2} - 2P_{1/2}$	1.5		
697.49	$3d^4 F_{3/2} - 2P_{3/2}$	0.5		
697.94	$3d^2 P_{1/2} - 2P_{1/2}$	0.8		
698.77	$3d^4 F_{5/2} - 2P_{3/2}$	1.6		
704.523	$3d^4 F_{3/2} - 2P_{1/2}$	1.1		
718.09	$4s^2 P_{1/2} - 2P_{3/2}$	3.8		
723.36	$4s^2 P_{3/2} - 2P_{3/2}$	18.0		
725.55	$4s^2 P_{1/2} - 2P_{1/2}$	7.5		
730.93	$4s^2 P_{3/2} - 2P_{1/2}$	2.7		
754.82	$3d^4 D_{5/2} - 2P_{3/2}$	1.0		
762.20	$3d^4 D_{3/2} - 2P_{1/2}$	0.5		
			32	

and $4d'^2S$ states at high energies.

It should be noted in connection with the figures and with the cross sections given in Table I that no corrections have been made for cascade. Further discussion of cascade effects is given in connection with the individual configurations.

A careful check was made using the tables of Striganov and Sventitskii¹³ to see if any interference effects might be occurring from lines of Ar III. These should not be significant at the excitation energy of 100 eV because all their thresholds are in excess of 60 eV. The only line which could be positively identified was the $690.17\text{-}\text{\AA}$ $3p^4^3P\text{-}3d^5D$ line. Two other lines appeared broadened (see Table I) but there were no listed Ar III lines which could have caused this effect. Possible Ar III contributions were therefore assumed negligible and neglected.

INDIVIDUAL CONFIGURATIONS

$3p^43d$ configuration

This configuration is particularly readily analysed because the states can only decay to the ground $^2P_{1/2,3/2}$ states. This means that the level cross sections are obtained directly from the measured line cross sections. This data has been tabulated in the second column of Table II.

The only significant cascade into the $3d$ levels will be from the $4p$ levels. In some cases it is possible to estimate the magnitude of this using measurements of Feltsan and Povch¹⁰ for $4p \rightarrow 4s$ and $4p \rightarrow 3d$ transitions together with the known

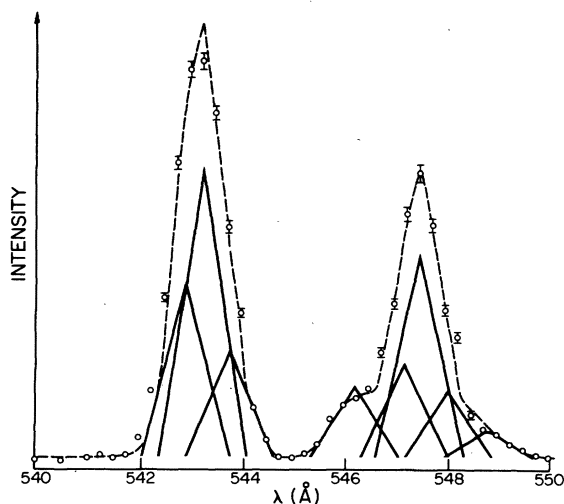


FIG. 2. Intensity-wavelength scan in the $542\text{--}550\text{-}\text{\AA}$ region. The dashed line, drawn through the experimental points, is the sum of the solid curves which indicate the contributions of the individual spectral features.

branching ratios^{8, 11, 12} for the $4p$ levels. Cascade corrected values have been tabulated in the third column of Table II. Cascade is seen to be especially significant for the 4D levels and also probably for the 4P levels though no measurements are available to check this.

One would expect direct excitation to populate the states within a given multiplet in the ratios of their statistical weights. The measured level cross sections when divided by the transition probability and the statistical weight should, therefore, be a constant. It is clear from the final column in Table II that this rule is closely observed for the 4F , 2D , and 2P multiplets. The error is rather larger in the case of 4D because of the very large cascade component. In the light of this evidence, it seems certain that direct excitation of the 4P states will be according to their statistical weights and so the large variation shown in the final column of Table II for this multiplet is almost certainly due to the effect of cascade.

The fact that such good agreement with expectations occurs is confirmation for the relative accuracy of Luyken's transition probabilities. However, when a detailed comparison is made between the experimentally measured relative transition probabilities for transitions to the two ground states from a common upper state, the agreement with the theoretical calculations is not so good in all cases. For example, although in the case of the $^2D_{3/2}$ upper state the relative transition probability to the $^2P_{3/2}$ and $^2P_{1/2}$ ground states is 0.20 compared with the Luyken's theoretical value of 0.18, for the $^2P_{3/2}$ and $^2P_{1/2}$ upper states the experimental ratios are 0.73 and 1.0, respectively, compared to theoretical values of 2.6 and 0.33. Clearly additional theoretical work is desirable here.

Figure 3(a) shows an excitation function for a pair of $3d$ levels. When compared with the other excitation functions it can be noted that the low-energy peak around 50 eV is much more pronounced. In general, the higher the excitation energy of the state the less pronounced this peak becomes supporting the conclusion that it is caused by autoionization effects whose significance will decrease as one goes to states of higher energy.

One notes also from Fig. 3(a) the expected negative slope of the Bethe plot at high electron energies.

$3p^44s$ and $3p^44s'$ configurations

The $3p^44s$ configuration has been dealt with in a previous publication⁵ and so no discussion will be included here except to comment that the relative intensity of two lines from a common upper level

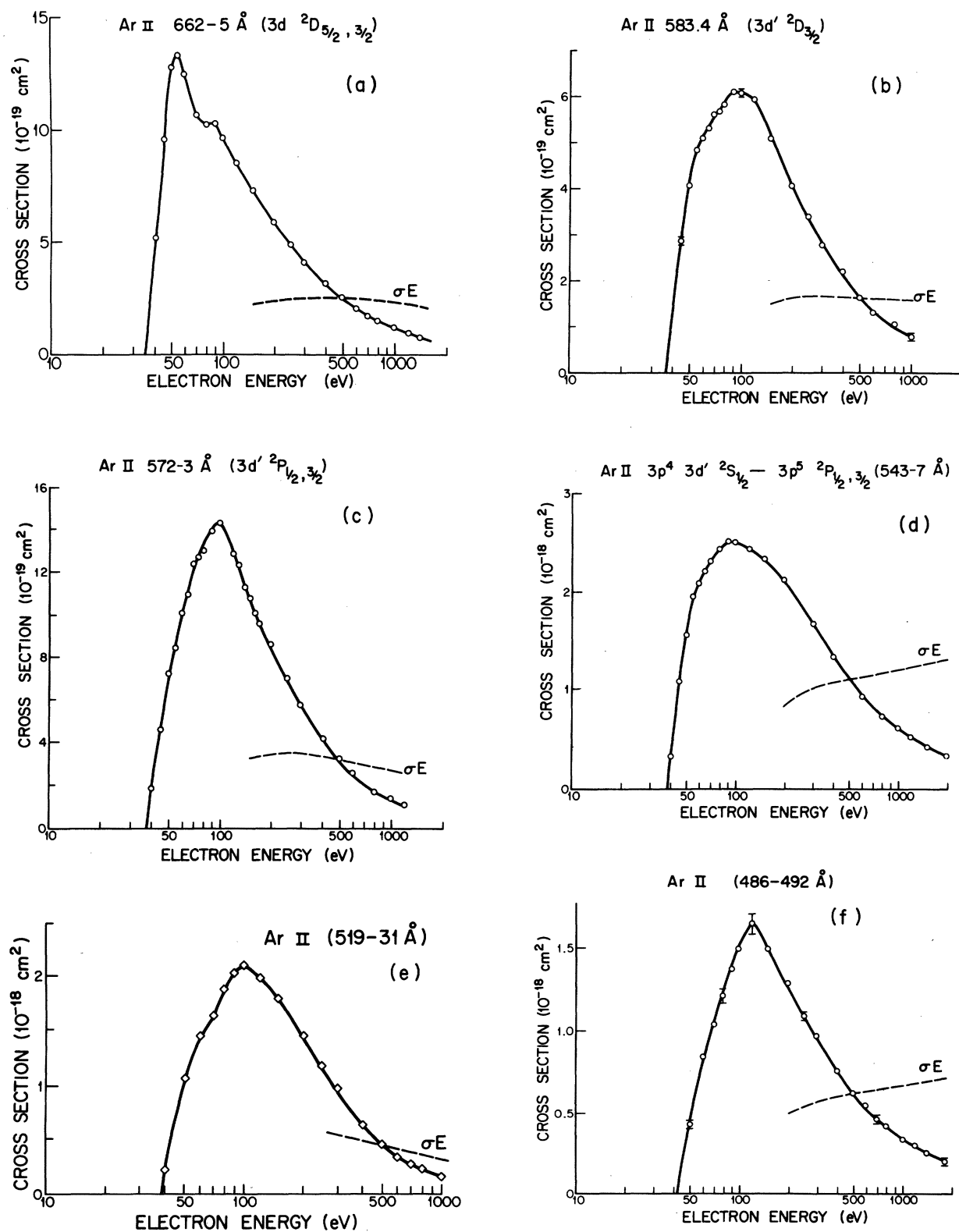


FIG. 3. (a)–(f) represents variation of apparent cross section of the spectral features indicated, as a function of exciting electron energy. Bethe plots are also shown.

to the two ground states agreed closely with Luyken's calculations and also that a very significant fraction [(40–70)%] of the excitation of the 4s levels occurred via cascade from the 4p levels.

Before any corrections for cascade were made the total 4s' cross section at 100 eV was 23.5×10^{-19} compared with a value of 32×10^{-19} for the 4s levels at the same energy. Using Feltsan and Povch's measurements for some of the $4p' \rightarrow 4s'$ cascading transitions together with branching ratios given by Luyken, it was possible to make some estimate of the fraction of 4s' excitation which was due to cascade. However, as no measurements have been reported for the $4p' \rightarrow 4s' \rightarrow 4s' \rightarrow 4s'$ cascading transitions, which are expected to be strong, only a lower limit to the cascade can be given. At 100 eV this is 25% for the ${}^2D_{5/2}$ level and 16% for the ${}^2D_{3/2}$ level. The $4s' \rightarrow 2D$ levels may be affected by configuration interaction with the $3d \rightarrow 2D$ levels as discussed later.

In contrast to the situation which exists for the 4s levels, there exists serious discrepancies with Luyken's calculations for the 4s' levels. Luyken does not consider the possibility of decay from $4s' \rightarrow 2D_{3/2}$ to the ${}^2P_{1/2}$ ground state. Table I shows that it is very strong, approximately 14 times stronger than the transition to the ${}^2P_{3/2}$ ground state (some uncertainty arises here because of blending with the $3d \rightarrow 4P_{1/2} \rightarrow 2P_{3/2}$ transition, but this is likely to be of the same order of magnitude as the transitions from the other 4P levels and therefore weak).

3p⁴3d' configuration

Numerical data for the individual transitions is given in Table I while Figs. 3(b)–3(d) illustrate the excitation functions obtained for states of different orbital angular momentum. The low-energy behavior (up to 100 eV) of the functions is similar in all cases but the high-energy behavior as demonstrated by the Bethe plots is distinctly different for the ${}^2S_{1/2}$ level due to the effects of configuration interaction as discussed more fully later.

The only possible transitions which might occur from the $3p^4 3d'$ levels, other than to the ground states, are to the 4p' states. These transitions would lie deep in the infrared. Luyken does not consider them in his theoretical transition probability calculations. We consider then that the level cross sections are given simply by the sum of the appropriate cross sections involving the ground-state configuration. These apparent level cross sections are listed in the second column of Table III. Cascade contributions to the apparent level cross sections from higher states are liable to be small at 100 eV because of the small cross sections for excitation of these states (using Feltsan and Povch's measurements for the 4p' levels and assuming an n^{-3} dependence of cross section with principal quantum-number results in cascading cross sections which are less than 10^{-19} cm². Hence cascade probably contributes less than 10% to the apparent level cross sections listed in Table III). Further justification for the

TABLE II. Data for 3p⁴3d configuration.

State	Measured level cross section at 100 eV (10 ⁻¹⁹ cm ²)	Corrected for cascade	Transition probability ^a (10 ⁸ sec ⁻¹)	$\sigma/[A(2J+1)]^b$ (10 ⁻²⁷ cm ² sec)
${}^4F_{5/2}$	1.6	1.36	0.014	16.2
${}^4F_{3/2}$	1.6	1.58	0.024	16.5
${}^4D_{5/2}$	1.0	0.24	0.0017	23.5
${}^4D_{3/2}$	0.5	0.09	0.00076	29.6
${}^4P_{3/2}$	1.3		0.045	4.8
${}^4P_{1/2}$	1.1		0.037	7.4
${}^2F_{5/2}$	0.5		0.045	5.6
${}^2F_{3/2}$	3.1		1.41	0.37
${}^2D_{5/2}$	8.5		16.7	0.08
${}^2D_{3/2}$	7.1		17.22	0.10
${}^2P_{3/2}$	2.6	2.17	0.348	1.55
${}^2P_{1/2}$	1.6	1.24	0.386	1.60

^aLuyken, Ref. 8.

^bWhen possible, σ is the cascade corrected cross section. Otherwise the measured cross section was used.

TABLE III. Data for the $3p^4 3d'$ configuration.

State	Measured cross section at 100 eV (10^{-19} cm 2)	A coefficient ^a (10^8 sec $^{-1}$)	$\sigma/[A(2J+1)](\times 10^{29})$	Branching ratio to ground states	
				Measured	Calculated ^a
$^2D_{5/2}$	13.3	159	1.39
$^2D_{3/2}$	9.55	148.3	1.61	0.57	0.43
$^2P_{3/2}$	15.85	210.8	1.88	3.59	3.32
$^2P_{1/2}$	7.9	208.6	1.89	0.52	0.58
$^2S_{1/2}$	12.0	244.6	2.45	1.5	1.79

^aLuyken, Ref. 8.

unimportance of cascade comes from column 4 of Table III where the apparent cross sections have been divided by the transition probabilities and statistical weights. Within a given multiplet this figure is approximately constant as one would expect.

The final two columns in Table III compare the experimental and theoretical branching ratios to the two ground states. The agreement with Luyken's calculations is seen to be good considering the possible error in the cross sections of some of the lines, for example, those from the $^2S_{1/2}$ level, due to overlap.

$3p^4 4d$ configuration

An excitation function covering the $4d$ states is illustrated in Fig. 3(e). In common with all the other functions it has a maximum around 100 eV with some structure at about 60 eV. The Bethe plot has the expected negative slope at high energy.

The second column of Table IV gives the total measured line cross sections for transitions from the $4d$ states to the ground states. Rudko and Tang¹² have calculated the lifetimes of the different states (from which the total transition probabilities can be obtained) and have also calculated the transition probabilities for the $4d-4p$ transitions. From these one can obtain the probabilities for transitions to the ground states. This gives the branching ratios listed in the third column of Table IV. Using these branching ratios, total

apparent level cross sections can be obtained. These are listed in the final column of Table IV. These cross sections seem to be anomalously high and one is forced to question seriously Rudko and Tang's branching ratios. However, even before taking account of the branching ratios, it is evident that these cross sections are considerably higher than those of the corresponding $3d$ states. This is anomalous as one normally considers that cross sections decrease with principal quantum number, usually to the inverse third power. Hence either the levels are being strongly populated by cascade from higher levels or else some mechanism is occurring leading to an enhancement of the cross sections.

No measurements or calculations exist which would allow an estimate of the fraction of the measured apparent cross sections which is due to cascade from higher levels. However it is unlikely that cascade excitation is very significant for the following reasons. Any such cascade will be predominantly from the higher np states with $n \geq 6$. The cross sections for excitation of these states should be well down on those of the $4p$ states and measurements^{10,14,15} have shown these to be of the order of 10^{-19} cm 2 or less. In addition, if significant population of higher np states was occurring then this would show up as anomalously high cascade excitation of other states, for example, $4s$, $5s$, or $3d$. This is not observed to be the case.

This leads to the conclusion that the anomalously

TABLE IV. Data for $3d^4 4d$ configuration.

State	Total measured line cross section from state at 100 eV (10^{-19} cm 2)	Branching ratio ^a	Apparent
			Level cross section (10^{-19} cm 2)
$^4D_{1/2}$	6.6	0.26	25.5
$^2D_{5/2}$	4.55	0.27	16.9
$^2D_{3/2}$	9.45	0.06	157.5
$^2P_{3/2}$	4.4	0.056	78.6
$^2P_{1/2}$	2.7	0.136	19.9

^aRudko and Tang, Ref. 12.

TABLE V. Data on $3p^4 5s$ configuration.

State	Total measured line cross section at 100 eV (10^{-19} cm ²)	Branching ratio ^a	Level cross section (10^{-19} cm ²)	$\sigma/[A(2J+1)]$ (10^{-27} cm ² sec)
$^2P_{3/2}$	2.0	0.33	6.1	0.48
$^2P_{1/2}$	4.1	0.76	5.4	0.70

^aRudko and Tang, Ref. 12.

large excitation of the $4d$ levels must be caused by some configuration-interaction effect probably with the $3d$ configuration leading to a transfer of excitation from these levels. This explanation is consistent with the work of Minnhagen⁷ and Luyken.⁸ Minnhagen points out that $3d^2P$ and $3d'^2P$ interact strongly as do $3d^2D$, $3d'^2D$, $3d''^2D$, $4s'^2D$, and $4d^2D$. Luyken⁸ has examined the situation more quantitatively and emphasizes the interaction between $3p^4 3d$ and the higher numbers of the same series in addition to $3p^4 3d'$. Because of the computational difficulties involved he was unable to take proper account of these interactions in his transition-probability calculations and hence he considers his calculated values for the $3d$ states to be subject to large errors (see also our previous comments in connection with the $3d$ configuration).

Unfortunately Luyken does not give details of the mixing coefficients involved but it is clear from examination of Tables II, III, and IV that much of the oscillator strength of the $3d$ states is being filtered off to $3d'$ and $4d$. Further calculations are desirable to help clarify these points.

From Table I the relative transitions probabilities to the $^2P_{3/2}$ and $^2P_{1/2}$ ground states from $4d^4D_{1/2}$, $4d^2D_{3/2}$, and $4d^2P_{1/2}$ states are 1.9, 0.93, and 0.5, respectively. These numbers will form a further test to future theoretical calculations.

$3p^4 5s$ configuration

The data concerning this configuration is summarized in Table V. Rudko and Tang¹² have calculated lifetimes and transition probabilities from which the branching ratio to the ground state was obtained. A considerable fraction of the excitation of the $5s$ states results in $5s-4p$ transitions. Using the calculated branching ratio results in a total apparent $5s^2P$ level cross section of 11.5×10^{-19} cm² at 100 eV. It is clear that cascade must be responsible for a significant fraction of the excitation otherwise there would be better agreement between the two terms in the last column of Table V. If a 30% cascade component is assumed, then the level cross section is approximately half the cascade corrected level cross section for the $4s^2P$ levels.⁵ This is

what would be expected assuming an n^{-3} dependence of cross section with principal quantum number. Again no theoretical calculations of the relative transition probabilities to the two ground states are available. The experimental values are 5.7 and 1.6 for the $5s^2P_{3/2}$ and $5s^2P_{1/2}$ states, respectively.

$3p^4 4d'$ and $3p^4 5d$ configurations

As a result of the extreme overlap within the $3p^4 5d$ configuration and between this configuration and $3p^4 4d'$ (see Table I) it is only possible to put estimates on the cross sections for the different levels. There are given in Table VI. The large cross section for $4d'^2S_{1/2}$ is due to configuration interaction with $3s3p^6^2S_{1/2}$ (see later). As in the case of $3p^4 3d$ and $3p^4 4d$ excitation of the $3p^4 5d^2D$ terms predominates over the 2P and other terms.

Figure 3(f) presents a combined excitation function for the 486-492 Å lines and it therefore includes contributions from both $4d'$ and $5d$ states. At high energies it will be dominated by $4d'^2S_{1/2}$ as discussed later.

Configuration interaction among the $^2S_{1/2}$ states

Although a strong interaction has been demonstrated to exist between the 2D states of the $3d$, $3d'$, $4d$, and $4s'$ configurations, it is overshadowed by the interaction between the $3s3p^6^2S_{1/2}$ and the $3s^2 3p^4 3d'$ and $4d'^2S_{1/2}$ states.

It was possible to get quantitative information on this interaction in the present instance first because of the distinctly different high-energy behavior of the $^2S_{1/2}$ excitation functions [see Figs. 3(d) and 3(f)] and secondly because of the fact that the $^2S_{1/2}$ levels are not complicated by significant

TABLE VI. Data for $4d'$ and $5d$ configurations.

State	Measured apparent cross section at 100 eV (10^{-19} cm ²)
$4d'^2S_{1/2}$	8.6
$5d^2P_{3/2}$	0.5
$5d^2P_{1/2}$	1.5
$5d^2D_{5/2,3/2}$	4.6

cascade, thus enabling the level cross sections to be obtained unambiguously. This information may be compared with Luyken's⁹ calculations and with other data obtained by different experimental techniques. Recently Weigold *et al.*¹⁶ have observed the mixing in coincidence studies of the scattered and ejected electrons when argon is ionized by electron impact and Spears *et al.*¹⁷ have demonstrated it to be present in x-ray photoelectron studies. A preliminary note on this comparison has already been published.¹⁸

It is important to consider the possibility of cascade into and out of the three levels under consideration. For $3s3p^6 2S_{1/2}$ the only possible transitions are to the ground states and the only possibly significant cascade into the level is from the $4p'^2 P$ states via the 1575- and 1560-Å lines. This was investigated by Luyken *et al.*⁹ and found to be negligible. Hence, no corrections for cascade need be applied and the $3s3p^6 2S_{1/2}$ level cross section can be taken simply as the sum of the cross sections for 920 and 932 Å.

For $3d'^2 S_{1/2}$ Luyken's calculations¹⁰ indicate that again the only depopulating transitions which need be considered are those to the ground states. Cascade into this state is also unlikely to be a problem because of the small cross sections of the states which would be involved. Further, any cascade contribution will fall off rapidly with energy because of the two-electron nature of the initial excitation. Hence, the $3d'^2 S_{1/2}$ level cross section is represented by the sum of the cross sections for 543 and 547 Å. A complicating feature which must be accounted for is possible contribution to the measured cross section from nearby lines (see Fig. 2 and Table I). Again this effect will decrease towards high electron energy. Quartet states show an especially rapid decrease in cross section with energy¹⁰ and so it is assumed that contributions from these states may be neglected at high energies. To correct for contributions from the 5s levels, it was assumed that the 5s excitation function was similar in shape to the 4s one measured previously.⁵ Background contributions were thus calculated to vary from 10% at 1 keV to 7% at 2 keV. The ratio of the $3s3p^6 2S_{1/2}$ and $3d'^2 S_{1/2}$ cross sections was found to reach a constant value of 4.15 above 1 keV as shown in Fig. 4.

Transitions from the $4d'$ state to states other than the $2P_{1/2,3/2}$ ground states are also probably insignificant. Only three were recorded by Minnhagen⁷ and these with low intensities. In the absence of any information we have assumed that the sum of the line cross sections for 487 and 491 Å gives the total $4d'^2 S_{1/2}$ level cross section. In the event of this assumption not being justified,

the level cross section would have to be increased by the appropriate amount. Table I indicates that overlap with adjacent lines is a serious problem at 100 eV. The significance will decrease as the electron energy increases for the reasons discussed previously. As a first approximation to this background contribution at higher energies the $5d$ excitation function was assumed to have the same shape as the $4d$ one, Fig. 3(e). This enabled background corrections of 15% at 1 keV and 10% at 1800 eV to be estimated. This process is open to some error, but it is thought that these contributions are reasonably accurate. The ratio of the $3s3p^6 2S_{1/2}$ and $4d'^2 S_{1/2}$ cross sections reached a constant value of 7.9 at energies exceeding 1 keV, Fig. 4.

The constancy of the cross-section ratios illustrated in Fig. 4, together with the positive slopes of the Bethe plots for all three levels is very positive evidence for the link between them.

Table VII gives the relative cross sections for excitation of the three levels (taken from our high-energy data) and compares these with Luyken's calculations and the other experimental data. A number of points are evident. Our data suggests that the contribution of $3d'$ to the 3s hole state is not as high as is indicated by Luyken's calculations whereas $4d'$ seems to be rather stronger. This conclusion seems to be supported by the x-ray photoionization data. Weigold *et al.* find a much larger contribution from the combined d' states than do Spears *et al.* or ourselves, though our error bars are too large to be definitive about

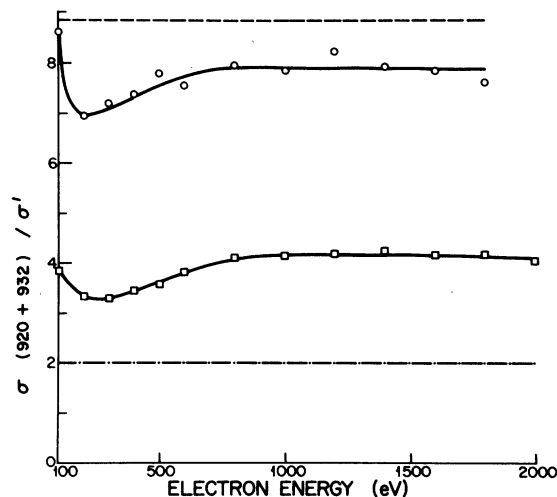


FIG. 4. Ratio of $3s3p^6 2S_{1/2}$ cross section $\sigma(920+932)$ to the $3s^2 3p^4 n d'^2 S_{1/2}$ cross sections σ' as a function of electron energy. Dashed line (----), $n=4$, Luyken (theory); (-o-o-), $n=4$, present work; (-□-□-), $n=3$, present work; dash-dot line (-·-·-), $n=3$, Luyken (theory).

TABLE VII. Relative cross sections of ${}^2S_{1/2}$ states.

State	Present work ^a			
	(electron impact)	Luyken ^b (theory)	Spears <i>et al.</i> (x-ray input)	Weigold <i>et al.</i> (<i>e-2e</i> experiment)
$3s3p^6$	100	100	100	100
$3p^43d'$	24_{-9}^{+13}	50	$(15-19) \pm 2^c$	72 ± 12^d
$3p^44d'$	12.7_{-4}^{+7}	11	$(6-8) \pm 3^c$	

^a Errors given in the present work are based on assumed errors of $\pm 20\%$ in the cross-section values. The slight difference between the values quoted here and in Ref. 18 should be noted. This is because no correction for high-energy background contributions was made in Ref. 18.

^b Luyken, Ref. 8.

^c Spears *et al.* (Ref. 17) found that their values depended slightly on x-ray energy.

^d Weigold *et al.* (Ref. 16) were unable to resolve the $3d'$ and $4d'$ states.

this discrepancy. Additional *e-2e* experiments with better energy resolution and also preferably carried out under conditions of low momentum transfer would clearly be of great value in resolving this question.

Note added in proof. Very recently J. Williams (private communication) has succeeded in resolving the $3d'$ and $4d'$ states in an *e-2e* experiment similar to that of Weigold *et al.* He finds the contributions from the two states to be of comparable intensity.

CONCLUSIONS

Cross-section data has been presented for the $4s'$, $5s$, $3d$, $4d$, $5d$, $3d'$, and $4d'$ configurations of Ar^+ . Except where configuration interaction with the $3s3p^6{}^2S_{1/2}$ state is occurring, the high-energy dependence of the cross sections is shown to be consistent with the dipole-forbidden, two-electron nature of the exciting transitions from

the Ar ground state. Where cascade could be properly taken into account, it was demonstrated that states of given orbital angular momentum and multiplicity were populated according to their statistical weights. In many cases significant discrepancies were observed between experimental relative transition probabilities and theoretical calculations, highlighting the need for additional more-refined theoretical work. Considerable evidence was uncovered for configuration-interaction effects. This caused considerable enhancement of the $3d'$, $4d'$, and $4d$ level cross sections. It was possible to make quantitative measurements of the mixing between $3s3p^6{}^2S_{1/2}$ and $3s^23p^43d'$ and $4d'{}^2S_{1/2}$. Discrepancies with theory and other experimental work were demonstrated.

ACKNOWLEDGMENT

It is a pleasure to acknowledge helpful discussions with P. J. O. Teubner.

*Work supported by the National Research Council of Canada.

¹A. Crowe, J. A. Preston, and J. W. McConkey, *J. Chem. Phys.* **57**, 1720 (1972).

²J. W. McConkey and J. A. Preston, *J. Phys. B* **6**, L138 (1973).

³J. W. McConkey and J. A. Preston, *Abstracts of the Eighth International Conference on Electronic and Atomic Collisions, Belgrade, 1973* (Institute of Physics, Belgrade, 1973), Vol. 1, p. 273.

⁴J. W. McConkey and F. G. Donaldson, *Can. J. Phys.* **51**, 914 (1973).

⁵K-H. Tan, F. G. Donaldson and J. W. McConkey, *Can. J. Phys.* **52**, 786 (1974).

⁶F. G. Donaldson, M. A. Hender, and J. W. McConkey, *J. Phys. B* **5**, 1192 (1972).

⁷L. Minnhagen, *Ark. Fys.* **25**, 203 (1963); **14**, 483 (1959).

⁸B. F. J. Luyken, *Physica* **60**, 432 (1972).

⁹B. F. J. Luyken, F. J. de Heer, and R. Ch. Baas, *Physica* **61**, 200 (1972).

¹⁰P. V. Feltsan and H. M. Povch, *Opt. Spektrosk.* **28**, 217 (1970) [*Opt. Spectrosc.* **28**, 119 (1970)].

¹¹J. B. Shumaker, Jr. and C. H. Popenoe, *J. Opt. Soc. Amer.*, **59**, 980 (1969).

¹²R. I. Rudko and C. L. Tang, *J. App. Phys.* **38**, 4731 (1967).

¹³A. R. Striganov and N. S. Sventitskii, *Tables of Spectral Lines of Neutral and Ionized Atoms* (Plenum, New York, 1968).

¹⁴I. D. Latimer and R. M. St. John, *Phys. Rev. A* **1**, 1612 (1970).

¹⁵P. N. Clout and D. W. O. Heddle, *J. Phys. B* **4**, 483 (1971).

¹⁶E. Weigold, S. T. Hood, and P. J. O. Teubner, *Phys. Rev. Lett.* **30**, 475 (1973).

¹⁷D. P. Spears, H. J. Fischbeck, and T. A. Carlson, *Phys. Rev. A* **9**, 1603 (1974).

¹⁸K-H. Tan and J. W. McConkey, *J. Phys. B* **7**, L183 (1974).